

## AN INNOVATIVE APPROACH TO FABRICATION WITH PHOTO-CURED RESINS BY SHELL-PRINTED-CORE-CASTING

Emil SZYMCZYK<sup>\*</sup>, Maciej REĆKO<sup>\*</sup>, Kazimierz DZIERŻEK<sup>\*</sup>, Karol SAPIOLKO<sup>\*</sup>

<sup>\*</sup>Faculty of Mechanical Engineering, Białystok University of Technology, ul. Wiejska 45C, 15-351 Białystok, Poland

[emil-szymczyk3@wp.pl](mailto:emil-szymczyk3@wp.pl), [m.recko@pb.edu.pl](mailto:m.recko@pb.edu.pl), [k.dzierzek@pb.edu.pl](mailto:k.dzierzek@pb.edu.pl), [karol@sapiolko.com](mailto:karol@sapiolko.com)

received 30 January 2023, revised 2 May 2023, accepted 3 May 2023

**Abstract:** Modified LCD-based method was used to print three-dimensional (3D) elements. This innovative method combines printing the external shell and filling, thus obtaining mould by casting resin. In order to compare the properties of prints obtained with this method with the ones fabricated in a standard procedure, we conducted bending tests of vertically/horizontally printed and shell-printed cast specimens. The shell-cast samples showed higher flexural strength and larger values of apparent Young's modulus. The presented results also concern the kinetics of curing samples obtained with different fabrication routes.

**Key words:** stereolithography, resin, printing, casting, curing, tensile test, bending

### 1. INTRODUCTION

Stereolithography (SLA) is one of the methods of three-dimensional (3D) printing that is based on a process of photopolymerisation (1). This method involves the use of a laser beam to cure a photopolymer liquid, layer by layer, into a solid object. The dimensional accuracy of elements printed with SLA is the main advantage of this method, and it is often used to create precise, intricate designs. However, a significant disadvantage of SLA is the poor mechanical properties of the product (2), which can be a major limitation in certain applications. SLA products have properties (3) that depend strongly on several factors such as the layer thickness, curing time during and post-curing time, printing temperature and fabrication orientation (4, 5). These factors can significantly affect the mechanical properties of the final product, such as its strength and durability. 3D printed elements, by definition, have layered structures and anisotropic properties along and across the layers, which means that the properties of the material vary in different directions.

On one hand, cast elements have isotropic properties (6), which means that the properties of the material are consistent in all directions. In some applications, this makes casting an attractive alternative to 3D printing. However, comparing the two methods, one should also consider the required processing time. Printing with laser technology can take up to several dozen hours. In contrast, the use of LCD printers significantly reduces this time, but cannot be viewed as a fast fabrication route, especially in comparison with casting. On the other hand, casting needs to be preceded by building the moulds, which might be time-consuming and require additional fabrication capacity.

Because of the above-given comments, we have put forward a hypothesis that an attractive alternative to 3D printing and casting can be a method combining these two. More precisely, we propose a two-step procedure: (a) printing of external shell of the element of interest and (b) casting resin to the thus printed shell/mould. This method allows for the creation of complex designs with high dimensional accuracy while also providing good

mechanical properties. The results of experiments described in the following sections demonstrate this method's advantages.

### 2. MATERIALS AND EXPERIMENTAL DETAILS

Elegoo Mars 2 desktop LCD-SLA printer was used as the primary equipment to fabricate the printed specimens in this study. This particular piece of equipment is quite popular among enthusiast-level customers, due to its ease of use and accessibility. LCD-SLA printers work by curing the resin layer using an LCD light source, illuminating the specimen cross-section (7). In this specific study, the layers in the prints were set at a thickness of 0.05 mm, with a curing time of 2.5 s for each layer.

The models for the specimens were designed using SolidWorks 2022® (Dassault Systèmes SolidWorks Corporation, USA) and then exported to a .stl file. Additional supports were added to the models using Formware 3D (Formware B.V. Amsterdam, Netherlands) to ensure the structural integrity of the printed specimens. The final step in the printing process involved slicing the files into G-code using CHITUBOX Software (CBD-Tech, China).

In this study, a transparent resin was used as it allows for the complete hardening of the resin. However, in order to conduct a thorough investigation, pigmented resins were also considered by incorporating black-coloured resin samples fabricated using the same printing parameters for comparison. The samples were cured for varying amounts of time, including 0 min, 2 min, 4 min, 8 min and 16 min (8). The resin supplier's data indicate that the tensile strength of the resin should be 23.4 MPa, with a Shore D hardness of 79. The recommended wavelength of curing light for this type of resin is 405 nm.

The geometry of the samples used in this study is shown in Figs. 1–3. The specimens were also printed in both horizontal and vertical orientations in order to further evaluate the impact of the printing orientation on the final specimens.

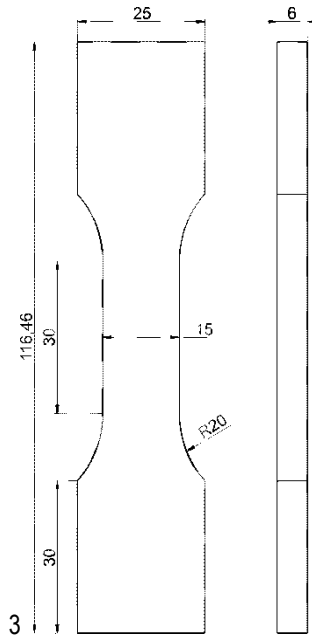


Fig. 1. Geometry of samples used in a uniaxial tensile test

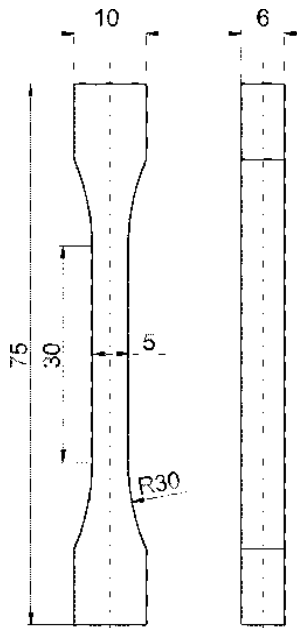


Fig. 2. Specimens used for testing flexural strength

In the case of print-cast samples, the resin was introduced into shells with a syringe. Special measures were taken to reduce the density of trapped air bubbles within the resin to mitigate their impact.

In order to conduct the three-point bend test, the samples were fabricated by being cast into an intricately designed mould. This mould, constructed out of plexiglass material, was explicitly created to expose the resin to the curing machine's light. In addition, the forms were tightly sealed using screw fastenings and plexiglass plates that were coated with multi-hydrocarbon sealant, ensuring a secure and reliable seal. A visual depiction of the casting sample preparation process is shown in Fig. 4.

During the production of cast samples, we encountered a significant obstacle in the form of air bubbles in the resin. We had to devise a method to overcome this issue (9), and after much

experimentation, we discovered that by reducing the pressure, we could effectively eliminate any air from the resin. To achieve this, we placed the moulds in a vacuum chamber (Fig. 5) during the pouring and hardening process, ensuring that the final product was free from any defects caused by air bubbles.

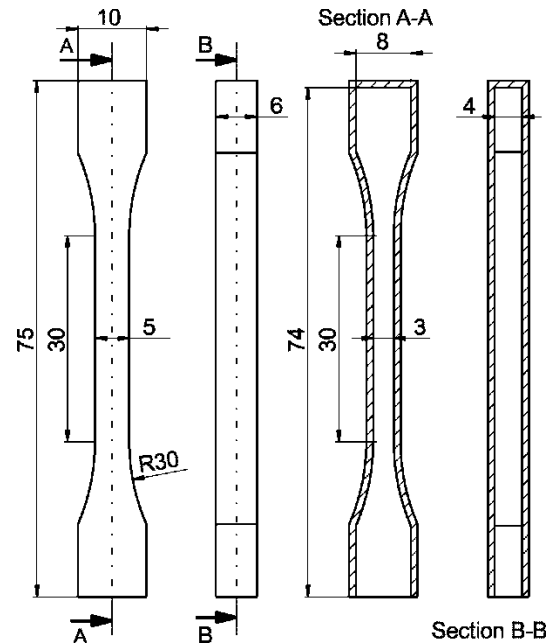


Fig. 3. Shells for shell-cast specimens



Fig. 4. Mould used for casting

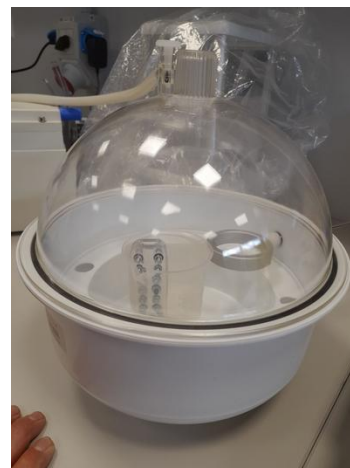


Fig. 5. Moulds with resin in a vacuum (de-gassed) chamber

Final curing was accomplished using Elegoo Mercury Plus Curing Station. The machine is equipped with sets of UV emitters. The light emitted by the light source is tuned to the wavelength required to cure this resin – 405 nm, and in addition, it has a set of UV-A emitting LEDs. The power of the light source, measured at the centre of the curing plate, was 220 W/m<sup>2</sup>. Since the light was obstructed during our studies by plexiglass and pre-cured resin, we measured the power provided to the resin at 180 W/m<sup>2</sup> and 23 W/m<sup>2</sup>, respectively. Based on the thermal imaging camera recordings, we obtained a temperature–time graph during the curing process, as shown in Fig. 6.

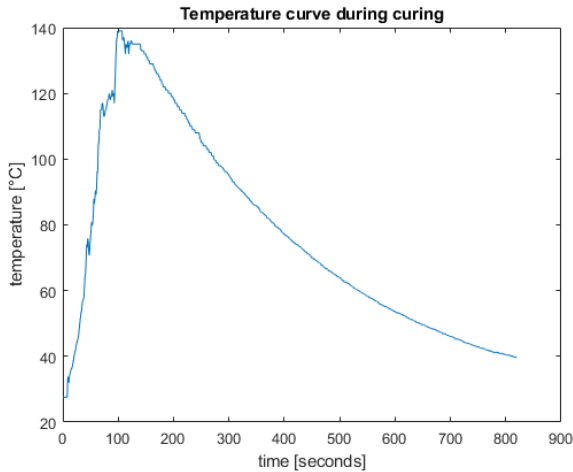


Fig. 6. Temperature profile of the tested sample

It can be noted that after 100 s, the sample reaches the maximum temperature of 140°C. It is much less than 180°C reported in “Mechanical property modelling of photosensitive liquid resin in SLA additive manufacturing: Bridging degree of cure with tensile strength and hardness. Materials & Design” (10). Nevertheless, the curing employed proved to provide sufficient strength to all samples. It should be noted that the temperature measurements in our case were performed on the surface of the specimen. This meant a 1 mm layer of pre-cured resin between the “heat source” and the sample’s surface.

The tensile tests were performed on a Zwick/Roell Z010 (11) testing machine, following the procedure described by (12). Engineering stress–strain curves were analysed to determine maximum engineering stress, elastic limit and apparent Young’s modulus based on the trend of linear parts of the curves. Aramis 3D 4M system was used to determine strain distributions along the gauge length of the specimens. The bending tests were carried out on the MTS Insight.

### 3. RESULTS

Results of the tensile tests are shown in Figs. 7 and 8 using the following description of the specimens:

- FVS – vertical,
- FHS – horizontal,
- FHSS – horizontal supports,
- FHBS – horizontal black.

The results of the bending tests are presented in Fig. 9 in the form of a bar plot of maximum bending forces. As determined from the bending test, apparent Young’s modulus values are

given in Fig. 10. As a test, we added two more cast samples with 60 min- and 90-min curing times to see if further curing would affect performance.

Results of the bending tests shown in Figs. 9 and 10 are using the following description of the specimens:

- FVS – vertical,
- FHS – horizontal,
- SHELL – printed shell filled with resin,
- CS – casted specimen.

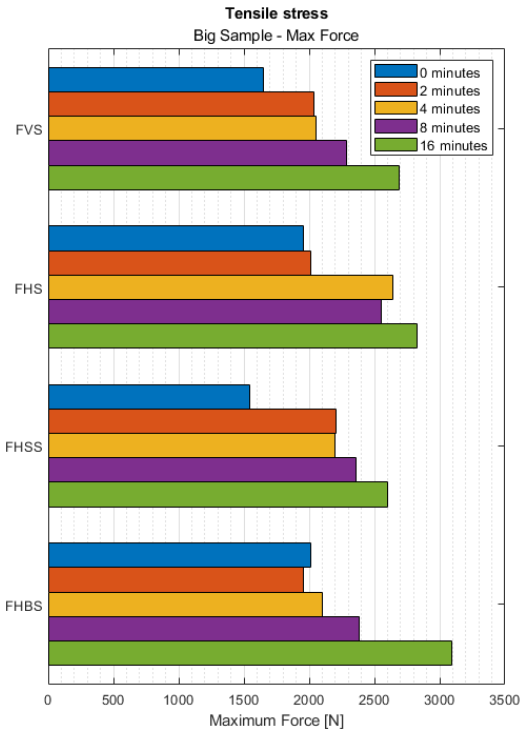


Fig. 7. Maximum engineering stress of the specimens

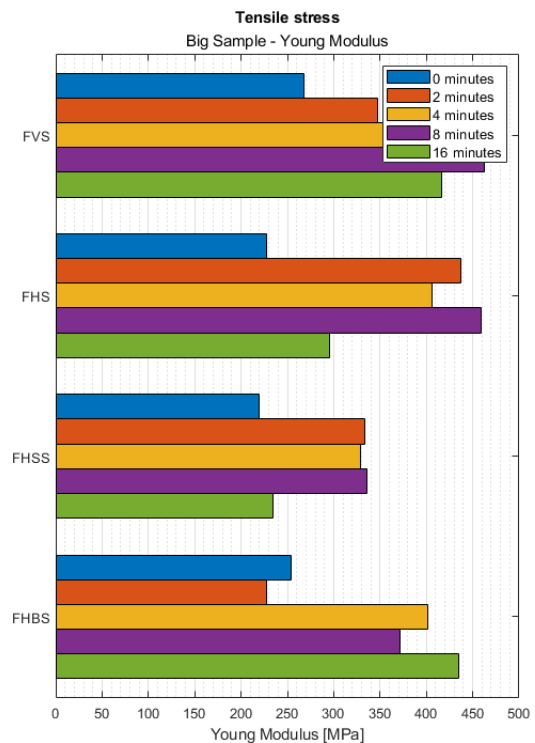


Fig. 8. Apparent Young’s modulus

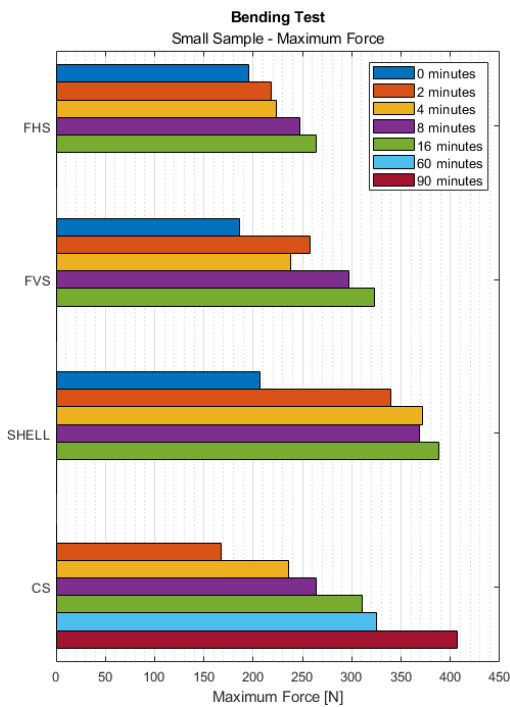


Fig. 9. Maximum bending forces of the studied specimens

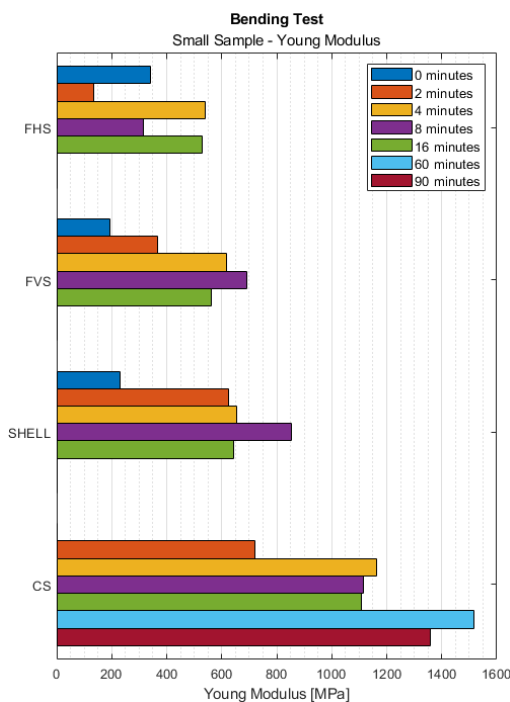


Fig. 10. Young's modulus determined based on a bending test

#### 4. DISCUSSION

The results obtained in this study provide useful insight into the properties of print-outs prepared with SLA LCD technology. However, we intend to focus the discussion on the properties of print-cast specimens, benchmarking them against the properties of the one obtained by printing/casting alone. In this context, bending tests have shown that the shell-cast samples have the highest flexural strength, 20% higher than the second-best result in our sample (vertical printed and cured for 16 min).

However, tensile tests have shown that horizontally printed samples without supports have the highest tensile strength. For example, after curing it for 16 min, the FHBS sample increased its tensile strength by 53.7%.

The results of our study indicate that cast specimens demonstrate the highest values of apparent Young's modulus. In contrast, shell-cast specimens exhibit a 26.77% lower Young's modulus in comparison to cast specimens. However, shell-cast specimens still display a 23.70% higher Young's modulus than the next best result, which is a sample printed vertically and cured for 8 min. Given that shell samples are easier to obtain than cast samples.

For SLA printers using a laser to print, this shell method can significantly reduce the time to receive the print. Comparing the time of obtaining the best samples, i.e. cast and shell, for the exemplary curing time of 16 min, the shell sample looks much better. Obtaining a cast sample consists of the following process: cutting the mould from plexiglass, tightening the mould screws, pouring, and curing the resin, and removing the sample from the mould. The entire process of obtaining one sample takes an average of 90 min. When removing the sample, we had to be careful not to damage the sample because the resin was sticking to the mould. However, making a shell sample involves printing the shell, pouring it and curing it. The entire process for one sample takes an average of 45 min.

A study conducted by Son et al. (12) explored a concept similar to our own, utilising ABS material for 3D-printed shells filled with epoxy resin. However, the study employed a different printing technique, FDM, and used a second material as a core cast. The scientists provided a detailed explanation of their multi-step procedure, which encompassed printing, shell treatment to enhance optimal casting and specimen curing. Their findings revealed that their samples exhibited an increase in mechanical properties in comparison to regular prints obtained with FDM printers, and at a higher manufacturing rate. In our opinion, their findings further indicate the viability of our manufacturing method.

Based on our observations, we have discovered a notable difference in the curing process for resin between moulds at the curing station and printed shell-cast samples. The reason for this discrepancy is likely due to the amount of energy delivered to the resin in each scenario. Specifically, while the energy delivered to print-cast samples is comparable to that of printed samples at 23 W/m<sup>2</sup> received from printer during manufacturing, cast samples inside a mould receive a significantly higher amount of energy, approximately eight times more. This ultimately leads to the entrapment of air bubbles within the resin. As part of our visual inspection process, we have rejected samples that exhibit excessive bubbles.

It should be noted that samples printed in black resin had similar mechanical parameters to those fabricated with transparent resin. UV curing time impacts the mechanical properties of the samples made of the resin used in this study, in agreement with the findings of (2, 13, 14). Furthermore, our results show that the curing time should be optimised for various fabrication methods and considering the elements' physical dimensions.

#### 5. CONCLUSIONS

The findings of the study indicate that the combination of printing and casting presents a viable alternative to employing

either technique in isolation. The mechanical characteristics of shell-printed-core-cast elements are akin to those of conventional castings, and in some instances, even surpass those of SLA prints. This approach holds the potential to reduce printing duration, as well as eliminate the requirement for casting moulds, while additionally providing superior polymerisation conditions that are congruent with the designated curing parameters.

However, it is important to note that to fully exploit this technology's potential, the curing conditions need to be optimised, depending on the shape and size of the product. This is because the size and shape of the product can greatly impact the curing process and ultimately affect the mechanical properties of the final product. Additionally, it is worth noting that the curing time plays an important role in the mechanical properties of the samples and should be considered when choosing the appropriate curing conditions.

In this research, we have gained valuable insights into the use of SLA LCD technology for printing purposes and the potential benefits of combining printing and casting techniques. This approach has demonstrated the ability to improve the mechanical properties of SLA prints while also reducing printing time, rendering it a suitable option for a range of applications. However, in order to optimise this approach, specific curing conditions must be tailored to the size and shape of the intended product.

## REFERENCES

- Dizon JRC, Espera AH, Chen Q, Advincula RC. Mechanical characterisation of 3D-printed polymers. *Addit Manuf.* 2018 Mar 1;20:44–67.
- Kazemi M, Rahimi A. Stereolithography process optimisation for tensile strength improvement of products. *Rapid Prototyp J.* 2018 Jan 1;24(4):688–97.
- Formlabs. Inc. Validating Isotropy in SLA 3D Printing [Internet]. FORMLABS WHITE PAPER Validating Isotropy in SLA 3D Printing. [cited 2022 Dec 19]. Available from: <https://3d.formlabs.com/validating-isotropy-in-sla-3d-printing/>
- Dulieu-Barton J m., Fulton M c. Mechanical Properties of a Typical Stereolithography Resin. *Strain.* 2000;36(2):81–7.
- Wang S, Ma Y, Deng Z, Zhang K, Dai S. Implementation of an elastoplastic constitutive model for 3D-printed materials fabricated by stereolithography. *Addit Manuf.* 2020 May 1;33:101104.
- Chacón JM, Caminero MA, García-Plaza E, Núñez PJ. Additive manufacturing of PLA structures using fused deposition modelling: Effect of process parameters on mechanical properties and their optimal selection. *Mater Des.* 2017 Jun 15;124:143–57.
- Schmidleithner C, Kalaskar D. Chapter 1 Stereolithography. In 2019 [cited 2023 Jan 19]. Available from: <https://www.semanticscholar.org/paper/Chapter-1-Stereolithography-Schmidleithner-Kalaskar/0af4e17637d487d284f9f15330572d555634fe81>
- Guttridge C, Shannon A, O'Sullivan A, O'Sullivan KJ, O'Sullivan LW. Impact of increased UV curing time on the curing depth of photosensitive resins for 3D Printing [Internet]. In Review; 2022 May [cited 2023 Jan 19]. Available from: <https://www.researchsquare.com/article/rs-1626243/v1>
- Tek-Tip: Reduce Bubbles in Clear Casting Resin [Internet]. Polytek Development Corp. [cited 2023 Jan 19]. Available from: <https://polytek.com/tutorial/tek-tip-reduce-bubbles-clear-casting-resin>
- Yang Y, Li L, Zhao J. Mechanical property modeling of photosensitive liquid resin in stereolithography additive manufacturing: Bridging degree of cure with tensile strength and hardness. *Mater Des.* 2019 Jan 15;162:418–28.
- ProLine universal testing machine [Internet]. ProLine universal testing machine. Available from: <https://www.zwickroell.com/products/static-materials-testing-machines/universal-testing-machines-for-static-applications/proline/>
- Petraşcu OL, Manole R, Pascu AM. The behavior of composite materials based on polyurethane resin subjected to uniaxial tensile test. *Mater Today Proc.* 2022 Jan 1;62:2673–8.
- Son J, Yun S, Park K, Ryu S, Kim S. Isotropic 3D printing using material extrusion of thin shell and post-casting of reinforcement core. *Addit Manuf.* 2022 Oct;58:102974.
- Dzadz Ł, Pyszczółkowski B. Analysis of the influence of UV light exposure time on hardness and density properties of SLA models. *Tech Sci [Internet].* 2020 Dec 9 [cited 2023 Jan 19];(2020). Available from: <https://czasopisma.uwm.edu.pl/index.php/ts/article/view/6119>
- Miedzińska D, Gieleta R, Popławski A. Experimental Study on Influence of Curing Time on Strength Behavior of SLA-Printed Samples Loaded with Different Strain Rates. *Materials.* 2020 Dec 21;13(24):5825.

Acknowledgement: The authors would like to thank K.J. Kurzydowski f or his fruitful discussions, guidance and support.

Emil Szymczyk:  <https://orcid.org/0009-0001-7242-2611>

Maciej Rećko:  <https://orcid.org/0000-0001-8768-3753>

Kazimierz Dzierżek:  <https://orcid.org/0000-0001-9184-1806>

Karol Sapiółko:  <https://orcid.org/0009-0000-8490-8582>



This work is licensed under the Creative Commons BY-NC-ND 4.0 license.